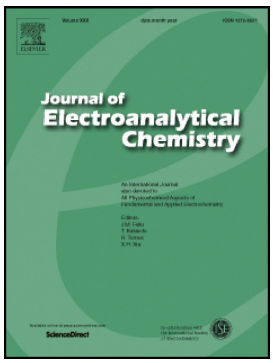


# Non-enzymatic sensor based on nitrogen-doped graphene modified with Pd nano-particles and NiAl layered double hydroxide for glucose determination in blood

Niusha Shishegari, Abbas Sabahi, Faranak Manteghi, Ali Ghaffarinejad, Zari Tehrani

PII: S1572-6657(20)30513-0

DOI: https://doi.org/10.1016/j.jelechem.2020.114285

Reference: JEAC 114285

To appear in: *Journal of Electroanalytical Chemistry*

Received date: 5 February 2020

Revised date: 7 May 2020

Accepted date: 22 May 2020

Please cite this article as: N. Shishegari, A. Sabahi, F. Manteghi, et al., Non-enzymatic sensor based on nitrogen-doped graphene modified with Pd nano-particles and NiAl layered double hydroxide for glucose determination in blood, *Journal of Electroanalytical Chemistry* (2020), https://doi.org/10.1016/j.jelechem.2020.114285

# Non-enzymatic sensor based on nitrogen-doped graphene modified with Pd nano-particles and NiAl layered double hydroxide for glucose determination in blood

Niusha Shishegari[a], Abbas Sabahi[b,c], Faranak Manteghi[a,*] f_manteghi@iust.ac.ir, Ali Ghaffarinejad[b,c,*] Ghaffarinejad@iust.ac.ir, Zari Tehrani[d]

[a]Department of Chemistry, Iran University of Science and Technology, Narmak, Tehran, Iran, 1684613114

[b]Research Laboratory of Real Samples Analysis, Faculty of Chemistry, Iran University of Science and Technology (IUST), Tehran, Iran, 1684613114

[c]Electroanalytical Chemistry Research Center, Iran University of Science and Technology (IUST), Tehran, Iran, 1684613114

[d]College of Engineering, Centre for NanoHealth, Institute of LifeScience-2, Swansea University, Singleton Park, Swansea, SA2 8PP, UK

[*]**Corresponding authors.**

## Abstract

Herein, a novel highly sensitive and selective non-enzymatic glucose sensor was developed. This sensor was prepared with a one-step electrodeposition process, which means that the palladium nanoparticles and NiAl layered double hydroxide were electrosynthesized simultaneously (Pd-NiAl-LDH) on a graphite sheet electrode (GS) covered by nitrogen-doped functionalized graphene (NFG). The sensing performance was investigated by linear sweep voltammetry (LSV), cyclic voltammetry (CV), electrochemical impedance spectroscopy (EIS) and chronoamperometry (CA) techniques. The results revealed that the one-step electrodeposition of Pd-NiAl-LDH nanocomposite on NFG provided a large surface area containing Ni and Pd electroactive centers and enhanced the electron transfer. This resulted in a remarkable effect on signal amplification toward glucose oxidation, with a wide linear range from 500 nM to 10 mM, an acceptable sensitivity of 315.46 μA. $cm^{-2}$. $dec^{-1}$ and a low detection limit of 234 nM based on a signal to noise ratio of 3. The relative standard deviation (RSD%) in all detection tests was lower than 5% and also the performance of fabricated GS/NFG/Pd-NiAl-LDH electrode which investigated in human real samples including serum, plasma and blood was acceptable, indicating the ability of the fabricated sensor in biological and clinical applications.


**Keywords:** One-step electrodeposition; Layered double hydroxide; Electrochemical non-enzymatic sensor; Glucose

## 1. Introduction

According to the World Health Organization (WHO), 422 million adults suffered from diabetes in 2014, compared to 108 million in 1980 [1] indicating that diabetes is presenting as a bigger and ever more pressing global health problem. Diabetes is a metabolic disease that results from the inability of the pancreas to produce or use insulin, also the complications of this global disease include but is not limited to heart attacks, strokes, kidney failure, leg amputation, vision loss and nerve damage [2]. It presents as a concern in all communities so the treatment process firstly needs to monitor and control glucose levels in

patients [3, 4]. Also, effective pre-diagnosis of diabetes like other diseases would hugely decrease the financial burden of its treatment for healthcare systems across the globe.

Amongst the various detection methods (chromatography, optical, thermometric, fluorescent, capillary zone electrophoresis, electrochemical and Fourier transform infrared spectroscopy) electrochemical techniques due to their high sensitivity, high selectivity, fast responses, low cost, ease of use and desirable detection limit, have been more attentive and progressive as a new successful technique between the detection methods [5, 6]. Electrochemical glucose sensors can be classified as non-enzymatic and enzymatic sensors. Non-enzymatic sensors have been developed to overcome the drawbacks of the enzymatic sensor (dependence of enzyme activity on pH, temperature, humidity, interference and lack of stability) [7, 8].

Various non-enzymatic glucose sensors have been utilized based on various types of materials include of metals (Pd, Pt, Au, Ni), metal oxides (NiO, CuO, $Co_3O_4$), alloys (Pt-Pd, Pt-Ni), complexes (cobalt phthalocyanine tetrasulfonate, nickel hexacyanoferrate), carbon-based electrode (carbon nanotubes, graphene, graphene oxides, nitrogen-doped graphene) [9] conductive polymers (polypyrrole, polyaniline) [10] and clay modified electrode (Layered double hydroxide (LDH), and zeolite) [11, 12].

Among the carbon-based materials, graphene has been more attentive and widely used. Graphene is a zero bandgap semiconductor and a monolayer of carbon atoms arranged in a honeycomb structure, which has special properties like high electrical conductivity, large surface area mechanical flexibility, and chemical and thermal stability [13, 14]. To harness the advantageous properties of graphene, the chemical-doping methods of carbon substrates with hetero atoms were used to modify properties such as improving the conductivity, controlling the surface structure and generating some special and also local chemical changes in the host material structure [15]. Nitrogen is a dopant for creating chemically active sites with catalytic properties that act as anchoring sites for metal and metal-oxide nanoparticle deposition [15]. Due to the special properties, graphene provides an ideal platform for electronics, electric devices, sensors and biosensors [16]. Among the different types of metallic nanoparticles that used for graphene-

modification, palladium nanoparticles (PdNPs) are the most efficient catalysts in the formation of C–C bond and chemical transformations such as hydrogenation, hydrodechlorination, carbonylation, and oxidation. Besides, the use of PdNPs in the glucose sensors effectively improved the sensitivity and selectivity toward the oxidation of glucose [16, 17].

Among the clay-based materials for glucose oxidation, LDHs have a wide range of applications due to the existence of metallic active centers in their structures [18]. Generally, the chemical composition of LDHs can be represented as $[M^{II}_{1-x}M^{III}_{x}(OH)_2]^{z+}A^{n-}_{z/n} \cdot H_2O$, where $M^{II}$ = divalent cations ($Mg^{2+}$, $Zn^{2+}$, $Ni^{2+}$, $Co^{2+}$, etc.); $M^{III}$ = trivalent cations ($Al^{3+}$, $Cr^{3+}$, $Fe^{3+}$, $Mn^{3+}$), and $A^{n-}$ = anions interlayers ($Cl^-$, $NO_3^-$, $ClO_4^-$, $CO_3^{2-}$, $SO_4^{2-}$), also these types of compositions can able to provides positively charged environment [19]. Due to the unique properties of LDHs such as layered structure, ionic exchange compatibility, high surface area, catalytic activity and low cost these materials are suitable candidates for electrochemical sensing devices [20, 21]. Through the special properties of NiAl-LDH, fast electron transport can be achieved due to the presence of nickel active sites in its structure that makes it particularly attractive to use in non-enzymatic glucose sensors.

Asadian et al. fabricated a non-enzymatic glucose sensor based on NiCo-LDH nanosheets/graphene-nanoribbons which modified glassy carbon electrode. Due to the preparation of high surface area by NiCo-LDH nanosheets and also the presence of more edge atoms in narrow graphene nanoribbons, which can serve as active sites for the electron transfer process, the fabricated sensor exhibited high sensitivity and fast amperometric responses toward glucose determination [22]. In another non-enzymatic glucose sensor, Wang et al. used Pd nanoparticles as an excellent catalyst on the active sites of graphene oxide (GO) surface for modification glassy carbon electrode. The prepared PdNPs/GO electrode showed a good catalytic performance in the determination of glucose in alkaline medium [23]. Eshghi et al. modified glassy carbon electrode by graphene/NiFe-LDH nano composites for study on electro-oxidation of glucose. The NiFe-LDH nanocomposite was electrosynthesized on graphene/GCE by a constant potential. Fabricated electrode studied the glucose electro-oxidation reaction through cyclic voltammetry,

chronoamperometry and electrochemical impedance spectroscopy (EIS) techniques in alkaline media. Results exhibited high catalytic activity, stability of the prepared graphene/NieFe LDH electrode toward glucose electro oxidation reaction under the effect of diffusion process [24]. Also, Fu et al. constructed another non-enzymatic glucose sensor based on AuNPs decorated on ternary NiAl LDH/single-walled carbon nanotubes (SWCNTs)/graphene nanocomposite which modified on GCE. The AuNPs were synthesis on surface of LDH/CNTs-G and the fabricated electrode (Au/LDH-CNTs-G/GCE) showed excellent electrochemical performance toward oxidation of glucose, due to synergic properties of Au NPs, LDH materials and carbon nanomaterials [25]. Therefore, the design and preparation of new types of material with high catalytic activity are of great importance for glucose non-enzymatic sensors fabrication.

In the present study, we report a novel non-enzymatic glucose sensor based on GS/NFG/Pd-NiAl-LDH, with GS being a graphite sheet, NFG being N-doped functionalized graphene and Pd-NiAl-LDH being palladium nanoparticles decorated on NiAl-LDH. On the first layer, the use of NFG resulted in an improvement in the electron transfer and prepared a large surface area for the electrodeposition of Pd-NiAl-LDH. The presence of Ni and Pd active centers in the structure of LDH caused to fast electron-transport and improved the catalytic activity of LDH in glucose oxidation. The fabricated GS/NFG/Pd-NiAl-LDH electrode not only has suitable stability, selectivity and sensitivity, but also exhibited an acceptable performance in real human samples such as blood, serum, and plasma.

## 2. Material and methods

### 2.1. Chemicals and reagents

Graphite powder (spectroscopic grade, particle size ≤ 50 μm), sulfuric acid ($H_2SO_4$, purity 98%), sodium nitrate ($NaNO_3$) and potassium permanganate ($KMnO_4$) as the reagents for graphene oxide (GO) preparation, nitric acid ($HNO_3$), potassium nitrate ($KNO_3$), nickel nitrate ($Ni(NO_3)_2{\cdot}6H_2O$), aluminum nitrate ($Al(NO_3)_3{\cdot}9H_2O$), palladium chloride ($PdCl_2$), sodium hydroxide (NaOH), potassium ferrocyanide

($K_4Fe(CN)_6$), ethylenediaminetetraacetic acid (EDTA), potassium ferricyanide ($K_3Fe(CN)_6$), glucose (Glu) and also all materials as interferences including uric acid (UA), dopamine hydrochloride (DA, purity 98%), ascorbic acid (AA), glycine (Gly), L-cysteine (L-cys) and cystamine (AED) were purchased from Merck company and used as received. Also, 1-Ethyl-3-(3-dimethylaminopropyl) carbodiimide hydrochloride (EDC, purity 98%), N-hydroxysuccinimide (NHS, purity 98%), phosphate-buffered saline (PBS) and dimethylformamide (DMF) were purchased from Sigma-Aldrich company and used as received. The GS electrodes were purchased from Latech Scientific Supply Pte Ltd (Singapore). The 0.01 mol. $L^{-1}$ solution of PBS (pH 7.4) containing equivalent molar concentrations (2.5 mmol. $L^{-1}$) of $K_3Fe(CN)_6$ and $K_4Fe(CN)_6$ probe salts were used as characterization electrolyte for layers. A 0.1 M NaOH solution was used as a sensing electrolyte and also all the aqueous solutions were made with ultrapure deionized water (DI).

### 2.2. Apparatus and methods

Voltammetric, amperometric, and EIS measurements were carried out with an Autolab Potentiostat/Galvanostat (PGSTAT204, Netherlands). The amperometric and voltammetric data were analyzed with Nova 1.11 software and the EIS data with ZSimpWin software (version 3.40). A standard three-electrode cell was used, including the modified GS as the working electrode, Ag/AgCl (3 M KCl) electrode as the reference and Pt rode as the counter electrode. The EIS measurements were made within the frequency range of $10^{-1}$ –$10^{5}$ Hz, with the potential amplitude of 10 mV around the open circuit potential ($E_{ocp}$) in the 2.5 mM solution of $[Fe(CN)_6]^{3-/4-}$ and 0.01 M solution of PBS. The characterization of the electrode surface morphology and elemental analysis was accomplished with the following techniques and instruments, Scanning Electron Microscopy (SEM; TESCAN/VEGA2, Czech Republic), Field Emission Scanning Electron Microscopy (FE-SEM) equipped with Energy-Dispersive X-ray Spectroscopy (EDS) (TESCAN MIRA3, Czech Republic). Also, X-ray photoelectron spectroscopy (XPS) measurements were performed with a Kratos Axis Supra XPS system with a monochromatic Al Kα X-ray source with an emission current of 15 mA.

### 2.3. Synthesis of NFG/Pd-NiAl-LDH nano-composite

In line with our previous work [26], firstly the graphene oxide (GO) was synthesized by a modified Hummer's method, then functionalization of the synthesized GO was done by using 400 µM EDC and 100 µM NHS solutions, which were prepared by continuously stirring in DI water overnight. To reduce the functionalized GO, DMF was used due to the release of carbon monoxide at the boiling point of DMF, which caused to produce NFG [26]. For the synthesis of LDH, the divalent and trivalent cations ($M^{II}/M^{III}$ ) were used with four types of molar ratios including 2/1, 3/1, 4/1, 5/1[27]. The electrodeposition of Pd-NiAl-LDH was carried out according to the literature [28] that the molar ratio of $M^{II}/M^{III}$ for LDH is the 3/1, with some change such as adding the PdNPs to NiAl-LDH structure through a one-step electrodeposition process. Briefly, the one-step electrodeposition on GS electrode which was modified by NFG was carried out by a cathodic reduction in a solution containing 1 mM $PdCl_2$, 0.12 M $Ni(NO_3)_2$, 0.04 M $Al(NO_3)_3$, 0.5 M $HNO_3$ and 0.15 M $KNO_3$ at a constant potential of -0.9 V vs. Ag/AgCl for 90 s.

### 2.4. Real human sample preparation

Blood samples were collected from a healthy individual*. To plasma preparation, around 10 mL blood was collected in blood collection tubes containing $K_2$EDTA and consequently deproteinized through centrifugation at 2000 rpm for 10 min at 4 °C, which resulted to extract approximately 4 mL of plasma and stored at –20 °C. The frozen plasma was thawed at room temperature prior to use. To serum preparation, the above procedure was repeated without the use of $K_2$EDTA in the blood collection tubes and also for the analysis of the blood sample, these samples were used without any extraction or preparation procedure. The standard addition method was carried out to monitoring the glucose levels in real human samples (blood, plasma and serum) which contains a certain amount of glucose and 0.1 M NaOH.

* One of the male authors of this study, aged between 25 and 30 years old, in the blood and oncology clinic of Ebnesina Hospital of Tehran, Iran.

### 2.5. Fabrication of GS/NFG/Pd-NiAl-LDH electrode

The fabrication process of the sensor is shown in Fig. 1. To eliminate the effects of any contamination during the electrochemical process, firstly GS electrodes were washed with acetone, ethanol, and DI water, respectively, and after that, a certain surface area ($0.5 \times 0.5$ $cm^2$) was provided on them. In the second step, to improve the electrical conductivity and also to prepare suitable surface area for the electrodeposition process, a certain volume of NFG (40 µL) with a concentration of 0.5 mg. $mL^{-1}$ was cast coated on GS electrodes. Finally, the Pd-NiAl-LDH film was prepared by using CA technique with a constant potential of –0.9 V vs. Ag/AgCl for 90 s as deposition time in 1 mM $PdCl_2$, 0.12 M $Ni(NO_3)_2$, 0.04 M $Al(NO_3)_3$, 0.5 M $HNO_3$ and 0.15 M $KNO_3$ solutions.

**Please insert Fig. 1 here.**

## 3.Results and discussions

### 3.1. Characterization of GS/NFG/Pd-NiAl-LDH electrode

XPS analysis was carried out to explore the nature of the existing elements and also prove the existence of Pd-NiAl-LDH on the modified electrode. As shown in the XPS spectrum of Pd/NiAl-LDH, the Pd *3d* XPS spectrum of GS/NFG/Pd-NiAl-LDH electrode (Fig. 2A), exhibits two peaks with binding energies at 335.6 and 340.9 eV which related to the Pd(0) $3d_{5/2}$ and Pd(0) $3d_{3/2}$, respectively. Also, two peaks at 337.7 and 342.7 eV were attributed to PdO $3d_{5/2}$ and PdO $3d_{3/2}$, respectively, that proves the presence of PdNPs in the NiAl-LDH structure [29]. About the Ni element, the XPS spectrum of Ni *2p* (Fig. 2B) shows two major peaks at 852.7 and 870.1 eV, which corresponds to Ni $2p_{3/2}$ and Ni $2p_{1/2}$ levels of $Ni^{+2}$, respectively. By observing the Al *2p* XPS spectrum (Fig. 2C), the peak at 74.5 eV attributed to

the presence of $Al^{+3}$ in the modified electrode [30]. These binding energy values indicated the presence of Pd, Ni, and Al elements and also prove the formation of Pd-NiAl-LDH on the fabricated electrode.

**Please insert Fig. 2 here.**

The surface morphologies of GS/NFG, GS/NFG/NiAl-LDH and GS/NFG/Pd-NiAl-LDH electrodes were characterized by SEM and FE-SEM. As shown in Fig. 3A, the surface of bare GS was covered by NFG at the first layer. The SEM image represents the graphene sheets that are placed at the top of each other to prepare a suitable surface area with enough roughness for interactions and additional modifications. Figure 3B, C show the FE-SEM images of NiAl-LDH layers on GS/NFG, that the NiAl-LDH film was grown horizontally and homogeneously on the surface of NFG. The deposition time has a significant influence on the morphology of NiAl-LDH layers, that short deposition times (60 s), caused to grow a few small LDH sheets on the NFG surface (Fig. 3B), but at 90 s (Fig. 3C), the small LDH sheets grew more and formed a denser LDH film which modified the NFG surface. As shown in Fig. 3D, E, F, that related to FE-SEM images of Pd-NiAl-LDH film at different scale, the thickness of the new LDH film was increased and caused the formation of a thicker film compared to NiAl-LDH film. Figure 3D, E, F indicate the Pd-NiAl-LDH film was grown uniformly and horizontally caused to form a denser film on the NFG surface, which represents a successful decoration of PdNPs between the NiAl-LDH layers. EDS and mapping analysis were used to determine the existence of elements and their distribution on the modified electrode surface. As shown in Fig. S1, the EDS chemical characterization result, describe the existence of carbon (C), oxygen (O), nickel (Ni), aluminum (Al) and palladium (Pd) on the electrode surface. In addition, the mapping analysis (Fig. 3G) indicates a uniform distribution of Ni and Al as LDH elements on the electrode surface and also shows the Pd distribution between the layers of NiAl-LDH.

**Please insert Fig. 3 here.**

### 3.2. Electrochemical investigation of GS/NFG/Pd-NiAl-LDH electrode

For the electrochemical investigation of the fabricated electrode, the LSV and EIS techniques were used. Two kinds of solutions including 0.01 M PBS containing 2.5 mM of $[Fe(CN)_6]^{3-/4-}$ as redox probe and the 0.1 M NaOH solution was used as supporting electrolytes. Different layers of the fabricated glucose sensor were investigated by the LSV technique in $[Fe(CN)_6]^{3-/4-}$ redox probe. As illustrated in Fig. 4A, the LSV curve of bare GS (curve a) as the first layer, had an increase at the current density of anodic peak ($j_{pa}$) due to the modifying by NFG (curve b). This increase in the $j_{pa}$ represents the unique properties of NFG, such as high surface area, excellent conductivity and catalytic properties that resulted in a suitable modification for the electrode. Furthermore, the NFG coating was used to prepare enough roughness for Pd-NiAl-LDH electrodeposition as the second layer. The high surface area of NFG provides excellent active sites on the electrode surface to interact with $[Fe(CN)_6]^{3-/4-}$ redox probe ions, which increases current density. After electrodeposition of NiAl-LDH on GS/NFG (GS/NFG/NiAl-LDH), the current density significantly decreased due to the low conductivity of the LDH layer (curve d), also, a positive shift at the anodic peak of $[Fe(CN)_6]^{3-/4-}$ was observed from the potential of 0.30 to 0.48 V. These positive shifts appear because of the nickel active center existence on the NiAl-LDH layers, which act as reversible electron redox points ($Ni^{III}/Ni^{II}$) that caused to make a positive shift around 0.48 V at anodic peak [28]. About the electrodeposition of NiAl-LDH on bare GS in the absence of NFG (GS/NiAl-LDH), the current density (curve c) was lower in comparison with the NFG presence (curve d). About the LSV curve of GS/NFG/Pd-NiAl-LDH electrode (curve f), the current density increased significantly due to the special properties of PdNPs such as improving the conductivity and catalytic activity of the final LDH film. Also about the absence of NFG in this simultaneous electrosynthesis (GS/Pd-NiAl-LDH) the current density (curve e) was lower compared to the presence of NFG (curve f) [29].

The EIS was performed to investigate the resistance of charge transfer ($R_{ct}$) for different layers of the modified electrode. The EIS measurements were carried out for all modified layers of the fabricated electrode in 0.01 M PBS solution containing 2.5 mM $[Fe(CN)_6]^{3-/4-}$ and in a frequency range from 50 mHz to 100 kHz at open circuit potential. The EIS data were plotted in the form of Nyquist plots (Fig. 4B). Randles equivalent circuit (*R*(*QR*)) was used for fitting the Nyquist plots of all modified layers, the related data were summarized in Table S1. Furthermore, the $R_s$ is related to the solution resistance, *CPE* or *Q* is the non-ideal capacitance that proves the roughness and heterogeneity of the surface and $R_{ct}$ is the resistance of charge transfer for electrode surface. By considering Fig. 4B and Table S1 data, the highest $R_{ct}$ (3765 Ω) was related to GS/NiAl-LDH, which shows a low charge transfer between the Ni active centers and the $[Fe(CN)_6]^{3-/4-}$ redox probe ions. After modifying the GS surface with NFG (GS/NFG/NiAl-LDH), an improvement in $R_{ct}$ (2840 Ω) was observed, which related to the high conductivity, large surface area and sufficient roughness of NFG that lead to decreases the $R_{ct}$ in comparison to GS/NiAl-LDH also improved the catalytic activity of NiAl-LDH. By adding PdNPs to the NiAl-LDH structure (GS/NFG/Pd-NiAl-LDH), a significant decrease was observed in $R_{ct}$ (1975 Ω) due to the unique properties of PdNPs such as excellent conductivity and high catalytic activity [31]. Furthermore, the presence of Ni and Pd active centers with the positive charge on Pd-NiAl-LDH surface led to electrostatic interaction with the negative charge ions of $[Fe(CN)_6]^{3-/4-}$ redox probe, that caused to decrease of $R_{ct}$ . The absence of NFG (GS/Pd-NiAl-LDH), caused to increase $R_{ct}$ to 2339 Ω in comparison to GS/NFG/Pd-NiAl-LDH electrode.

**Please insert Fig. 4 here.**

### 3.3. Electrocatalysis of GS/NFG/Pd-NiAl-LDH electrode toward the glucose sensing

Electroactivity and conductivity of the different layers were determined by a 0.1 M NaOH solution, containing 10 mM of glucose. For this reason, the CV, LSV, and CA techniques were performed over the potential ranges of 0.2 to 0.8 V and -0.2 to 0.95 V at a scan rate of 20 $mV.s^{-1}$, for LSV and CV, respectively. The CA technique was performed at an optimized applied potential of 0.5 V for 130 s. As shown in Fig. S2A, after modifying bare GS with NFG (GS/NFG) due to the chemical stability and lack of active centers on the NFG surface, no obvious peaks were observed in the LSV of the GS/NFG electrode (curve a) in 0.1 M NaOH solution containing 10 mM of glucose. By modifying the GS/NFG surface with NiAl-LDH (GS/NFG/NiAl-LDH), an oxidation peak appeared around the potential of 0.48 V, which could be attributed to the oxidation of electroactive Ni centers ($Ni^{III}/Ni^{II}$) which act as a mediator for the glucose oxidation reaction (curve c). By direct electrodeposition of NiAl-LDH on GS (curve b), the density of glucose oxidation was decreased compared to curve c, which highlights that the presence of NFG substrate plays an important role in the preparation of adequate surface area for deposition of electroactive Ni centers which improves the electrode conductivity. Also, the NFG has edge planes which promote the charge transfer of glucose oxidation and caused to a synergistic effect with the LDH layer. The LSV of GS/NFG/Pd-NiAl-LDH (curve e) shows that adding PdNPs as an electroactive nanomaterial to the structure of NiAl-LDH caused a significant increase in $j_{pa}$. The presence of Pd caused to appear a synergic effect with NiAl-LDH which enhanced the electroactivity and electron transferring in NiAl-LDH [29]. In Fig. S2A, the curve d which is related to GS/Pd-NiAl-LDH electrode shows that $j_{pa}$ is gradually decreased in comparison to GS/NFG/Pd-NiAl-LDH electrode (curve e) due to the absence of NFG. The NFG substrate through the preparation high surface area caused to generate a large number of electroactive Ni centers. The performance of GS/NFG/Pd-NiAl-LDH in 0.1 M NaOH solution containing 10 mM of glucose, shows a clear increase in $j_{pa}$ that indicates the existence of a suitable and electroactive modified electrode_for glucose oxidation. In addition, the presence of Pd in the LDH structure increases the adsorption of $OH^-$ ions, which efficiently improves the oxidation of glucose. Figure S2B is attributed

to the CV of the modified electrode in a 0.1 M solution of NaOH in the absence of glucose. According to Fig. S2B, the curve a shows CV of GS/NFG layer in the alkaline solution, also all CVs show a visible Faradaic process that indicates a formal potential at 0.5 V which is related to the NiAl-LDH. By comparing the curves b and c which are related to the CVs of GS/NFG/NiAl-LDH and GS/NFG/Pd-NiAl-LDH respectively, an increase in the current density of anodic and cathodic peaks was observed at curve c, which is related to the presence of PdNPs in LDH structure. CV and LSV tests approve each other and also show the influence of Pd presence on accelerating the electron transferring and enhancing the electroactivity of NiAl-LDH to the oxidation of glucose. CA is a more sensitive technique and it was performed to investigate the performance and stability of the electrode modified layers. Figure S2C shows the typical amperometric response of the modified layers in 0.1 M NaOH solution containing 10 mM glucose at the applied potential 0.5 V for 130 s. As shown in Fig. S2C, the amperometric response for the first modified layer GS/NFG has the lowest $j$ compared to other layers, due to the absence of Ni and Pd active centers. By modifying the electrode surface with NiAl-LDH and Pd-NiAl-LDH, the current density significantly increased in the following order: GS/NFG/Pd-NiAl-LDH > GS/Pd-NiAl-LDH > GS/NFG/NiAl-LDH > GS/NiAl-LDH > GS/NFG in 0.1 M NaOH solution in the presence of glucose. The CA response of the fabricated electrode (GS/NFG/Pd-NiAl-LDH) shows a clear increase in $j$ rather than other modified electrodes and also indicates the sensitivity toward the presence of glucose.

### 3.4. Optimization of the experimental conditions

To enhance the performance of the fabricated sensor, the effect of some parameters including scan rate, pH value, and applied potential were investigated.

#### 3.4.1. Effect of scan rate

The effect of scan rate ($\upsilon$) on the $j_{pa}$ in glucose oxidation was investigated by LSV in 0.1 M solutions of NaOH containing 10 mM glucose, illustrated in Fig. 5A. It is clear that by increasing $\upsilon$ (10 – 200 mV. $s^{-1}$), the $j_{pa}$ increased and also a little positive shift at the glucose oxidation potential ($E_{pa}$) was observed [32]. The plot of $j_{pa}$ vs. $\sqrt{\upsilon}$ (Fig. 5B) represents an acceptable linear range with $R^2$ = 0.992, which indicates

the ability of the diffusion process over the GS/NFG/Pd-NiAl-LDH electrode. All LSV tests were done at 20 mV. $s^{-1}$ as determined scan rate.

### 3.4.2. Effect of pH value

The pH of the supporting electrolyte directly affected the performance of the fabricated sensor. This parameter was investigated at five different pH values (7.4, 9, 10, 11, 13) through the CA technique at the applied potential of 0.5 V for 130 s and also by LSV with a scan rate of 20 mV. $s^{-1}$ in the solution of PBS containing 10 mM of glucose. As shown in Fig. 5C, D, by increasing the pH value, the current density of glucose oxidation peak is significantly increased, which indicates suitable oxidation of glucose on GS/NFG/Pd-NiAl-LDH electrode and represents the proper activity of glucose in alkaline solutions [33]. The Ni centers which exist in the structure of LDH, form two types of crystallographic species in alkaline media, the hydrated $\alpha$-$Ni(OH)_2$ and the anhydrous $\beta$-$Ni(OH)_2$. The alkaline media caused to activate the Ni centers on LDH structure, also the oxidation of small organic molecules on the Ni centers occurs after the formation of Ni(III) species that form a radical intermediate [33]. Furthermore, due to the unstable state of LDH structures in acidic media (acidic media cause to damage LDH structure), these pH values were not examined. According to this study, the optimum pH for the suitable performance of the sensor was 13, therefore for the rest of experiments instead of PBS, the 0.1 M NaOH solution with a pH of 13 was used as the supporting electrolyte.

### 3.4.3. Effect of the applied potential

At amperometric sensing, the applied potential directly affected the oxidation current response. Due to the importance, the applied potential of the fabricated sensor was investigated in 0.1 M NaOH solution containing 10 mM glucose at different potentials from 0.4 to 0.6 V. The Fig. 5E, F illustrate the amperometric response of the GS/NFG/Pd-NiAl-LDH electrode in the presence of glucose. It is clear that the current density of glucose oxidation at 0.5 V potential was higher than other applied potentials and considered as the optimized potential.

**Please insert Fig. 5 here.**

### 3.5. Voltammetric and amperometric detection of glucose

Both LSV and CA techniques were utilized to ascertain the detection limit of glucose at the optimum condition. Figure 6A, B respectively show the voltammograms and calibration plot of glucose, which were sensed by the LSV technique in 0.1 M NaOH solution with a scan rate of 20 mV. $s^{-1}$, in different concentrations of glucose ($C_{Glu}$) varying from 100 µM to 10 mM. As shown in Fig. 6B, the fabricated GS/NFG/Pd-NiAl-LDH electrode has an acceptable performance toward glucose detection and the calibration plot presents a linear relationship for the modified electrode. According to Fig. 6B, the regression equation was $\Delta j$ = 73.418 $C$ + 377.81, with the correlation coefficient $R^2$ = 0.9913, which is also has a remarkable high sensitivity of 73.418 µA. $mM^{-1}.cm^{-2}$ and an acceptable experimental detection limit of 100 µM. The prominent glucose electrooxidation behavior on the fabricated electrode by LSV offered an excellent platform for sensing the low concentration of glucose through the CA technique due to its sensitivity rather than LSV.

**Please insert Fig. 6 here.**

The single-potential step chronoamperometry was employed to sense the low concentrations of glucose at the fabricated electrode (GS/NFG/Pd-NiAl-LDH). Chronoamperograms were recorded in 0.1 M NaOH solution under the optimum condition with different concentrations of glucose from 500 nM to 10 mM. Figure 6C, D respectively show the chronoamperograms and calibration plot of glucose sensing

by CA. In addition, the steady-state current that was recorded at 80 s, was related to the concentration of glucose. The regression equation has a semi-logarithmic linear relation with glucose concentration ($\Delta j$ = 315.46 log $C_{Glu}$ + 1092.7) with $R^2$ = 0.9964 as the correlation coefficient. Furthermore, the amperometry response represents a wide linear range from 500 nM to 10 mM with an acceptable sensitivity of 315.46 μA. $cm^{-2}$. $dec^{-1}$ and also the limit of detection (LOD) for glucose was found to be 234 nM, which was estimated by the LOD = 3(S/N) equation. For both the calibration plots (by LSV and CA), three distinct measurements were carried out by three fabricated electrodes (n = 3) and the relative standard deviation (RSD%) for each concentration was lower than 5%. In Table 1, the performance of the proposed modified electrode for glucose oxidation is compared to other electrodes based on LDH. According to Table 1, the fabricated electrode (GS/NFG/Pd/NiAl-LDH) has a wider linear range and a proper detection limit in comparison to similar studies.

**Table 1** Comparison of the sensing characteristics of several Ni-based non-enzymatic glucose sensors

| Electrode | Sensitivity ($\mu A.mM^{-1}.cm^{-2}$) | Linear range (mM) | LOD (nM) | Reference |
|---|---|---|---|---|
| Au/NiAl-LDH-CNTs-G/GCE | 1989 | 0.01-6.1 | 1000 | [25] |
| NiNPs/NiCo-LDH/GCE | 1235 | 0.005-14.8 | 1600 | [34] |
| NiAl-LDH/CC | 14130 | 0.001-0.329 | 220 | [35] |
| NiAl-LDH/Ti foil | 24.45 | 0.005-10 | 500 | [36] |
| NiFe-LDH/NF | 3680.2 | Up to 0.8 | 590 | [37] |
| NiAl-LDH/CHT/GCE | 309 | 0.01-10 | 10000 | [38] |
| NiCo-LDH/AgNW/GCE | 71.42 | 0.002-6 | 660 | [39] |
| NiCo-LDH@PPy/GCE | 46.04 | 0.05-8.2 | 31200 | [40] |
| $NiFe_2O_4$@NiCo-LDH@rGO/GCE | 111.86 | 0.035-4.525 | 12940 | [41] |
| GS/NFG/Pd/NiAl-LDH | 315.46 (μA. $cm^{-2}$. $dec^{-1}$) | 0.0005-10 | 234 | This work |

Abbreviations: G: graphene, CNTs: carbon nanotubes, GCE: glassy carbon electrode, NPs: nanoparticles, CC: carbon cloth, NF: nickel foam, GO: graphene oxide, NFG: nitrogen-doped graphene, NW: nano wire, PPy: polypyrole, rGO: reduced graphene oxide, GS: graphite sheet

### 3.6. The interference study

The selectivity of the sensors is an important parameter on the reliable performance of the sensing process. Consequently, the effect of some important molecules including AA, UA, DA, AED, L-Cys, and Gly were investigated on the fabricated sensor. The CA was employed under the optimum conditions in 0.1 M NaOH solution through the continuous stirring for the injection of 20 µL from each of the interferences with a concentration of 3 mM within 20 s (the first volume of the electrolyte solution was 5mL). As shown in Fig. 7A, the oxidation current response for each of the interferences was less than 10% in comparison to the glucose target, indicates a reliable selectivity of the fabricated sensor.

### 3.7. Real sample study

To investigate the potential of the fabricated sensor to monitor glucose levels in diabetic patients, the CA responses were recorded in real biological human samples. According to the procedure mentioned in section 2.4, subsequent to preparation of real human samples, the CA technique was carried out under the optimum conditions in 5 mL of serum, plasma, and blood containing 0.1 M NaOH (pH = 13) in the presence of two different concentrations of glucose (1 and 3 mM). It should be noted that the $j$ recorded at 80 s was related to the concentration of glucose. As shown in Fig. 7B, the recovery values of glucose obtained by the standard addition method for the real samples ranged from 90% to 111% (n = 3, RSD < 2%). The lowest recoveries were related to the blood samples, due to the complex matrix of blood rather than serum and plasma samples. Despite these, the fabricated sensor still exhibited an acceptable performance in each of the samples so it could be used in clinical application with the aim of pre-detection of diabetes.

**Please insert Fig. 7 here.**

### 3.8. Repeatability, reproducibility and stability of fabricated glucose sensor

The reproducibility of the proposed sensor (GS/NFG/Pd-NiAl-LDH) was characterized by measuring the five equally fabricated electrodes in the same conditions, through the CA by recording the glucose oxidation response at 80 s in 0.1 M NaOH solution containing 10 mM glucose (Fig. S3A). The calculated RSD value was less than 3%. Also, for examining the repeatability, the CA was used in 0.1 M NaOH solution under the stirring condition for 5 injections of 3 mM glucose with the volume of 20 µL (the first volume of electrolyte was 5 mL). According to Fig. S3B, by during the time and several injections of glucose, the current density of glucose oxidation had acceptable stability, indicating proper repeatability of the fabricated sensor with the RSD value that was less than 4%.

The long-term stability of the fabricated sensor is an important parameter in the process of detection and in the commercialization ability. Due to the importance, the stability of the sensor was investigated by the CA through recording the oxidation response of 10 mM glucose every 5 days and after 30 days, the sensor showed about 90% of its initial response current (Fig. S3C). The stability of the sensor at every period of time was acceptable and indicates the stability of the fabricated electrode (GS/NFG/Pd-NiAl-LDH).

## 4. Conclusions

In summary, a highly sensitive and selective non-enzymatic glucose sensor based on GS/NFG/Pd-NiAl-LDH electrode was successfully fabricated. The sensor showed superior catalytic performance for oxidation of glucose with a remarkable high sensitivity of 315.46 µA. $cm^{-2}$. $dec^{-1}$, a suitable selectivity in the presence of various interferences, a wide linear range of 500 nM to 10 mM and a low detection limit of 234 nM, which could be mainly attributed to the Ni and Pd active centers that caused to greater

electron transfer passages. The performance of the fabricated sensor in real human samples (serum, plasma, and blood) as a complex matrix was acceptable and indicates the potential applications of the sensor in clinical diagnosis and monitoring glucose level in the early stages of diabetes.

## Acknowledgment

The authors gratefully acknowledge the financial support of this work from Iran University of Science and Technology. They would like to thank Muhammad Munem Ali from the Centre of NanoHealth, Swansea University, Singleton Campus, Swansea, SA2 8PP, UK, for his assistance in XPS spectra of this work. This work was supported by the Welsh Government and European Commission under European Regional Development Funds (ERDF) through Sêr Cymru II Fellowships (Project Number: 80761-su-100).

## Appendix A. Supplementary data

## References

[1] W.H. Organization, World health statistics 2016: monitoring health for the SDGs sustainable development goals, World Health Organization2016.

[2] A.D. Association, Diagnosis and classification of diabetes mellitus, Diabetes care 33(Supplement 1) (2010) S62-S69.

[3] B.J. Van Enter, E. Von Hauff, Challenges and perspectives in continuous glucose monitoring, Chem. Commun. 54(40) (2018) 5032-5045.

[4] I. Lee, N. Loew, W. Tsugawa, C.-E. Lin, D. Probst, J.T. La Belle, K. Sode, The electrochemical behavior of a FAD dependent glucose dehydrogenase with direct electron transfer subunit by immobilization on self-assembled monolayers, Bioelectrochemistry. 121 (2018) 1-6.

[5] W.-C. Lee, K.-B. Kim, N. Gurudatt, K.K. Hussain, C.S. Choi, D.-S. Park, Y.-B. Shim, Comparison of enzymatic and non-enzymatic glucose sensors based on hierarchical Au-Ni alloy with conductive polymer, Biosens. Bioelectron. 130 (2019) 48-54.

[6] C. Zhang, Z. Zhang, Q. Yang, W. Chen, Graphene- based Electrochemical Glucose Sensors: Fabrication and Sensing Properties, Electroanalysis. 30(11) (2018) 2504-2524.

[7] M. Usman, L. Pan, A. Farid, S. Riaz, A.S. Khan, Z.Y. Peng, M.A. Khan, Ultra-fast and highly sensitive enzyme-free glucose sensor based on 3D vertically aligned silver nanoplates on nickel foam-graphene substrate, J. Electroanal. Chem. 848 (2019) 113342.

[8] T. Yang, J. Xu, L. Lu, X. Zhu, Y. Gao, H. Xing, Y. Yu, W. Ding, Z. Liu, Copper nanoparticle/graphene oxide/single wall carbon nanotube hybrid materials as electrochemical sensing platform for nonenzymatic glucose detection, J. Electroanal. Chem. 761 (2016) 118-124.

[9] K. Tian, M. Prestgard, A. Tiwari, A review of recent advances in nonenzymatic glucose sensors, Mater. Sci. Eng. C. 41 (2014) 100-118.

[10] M.H. Naveen, N.G. Gurudatt, Y.-B. Shim, Applications of conducting polymer composites to electrochemical sensors: a review, Appl. Mater. Today. 9 (2017) 419-433.

[11] D.-W. Hwang, S. Lee, M. Seo, T.D. Chung, Recent advances in electrochemical non-enzymatic glucose sensors–a review, Anal. Chim. Acta. 1033 (2018) 1-34.

[12] G. Wang, X. He, L. Wang, A. Gu, Y. Huang, B. Fang, B. Geng, X. Zhang, Non-enzymatic electrochemical sensing of glucose, Mikrochim. Acta. 180(3-4) (2013) 161-186.

[13] Y. Zhu, M.D. Stoller, W. Cai, A. Velamakanni, R.D. Piner, D. Chen, R.S. Ruoff, Exfoliation of graphite oxide in propylene carbonate and thermal reduction of the resulting graphene oxide platelets, ACS. Nano. 4(2) (2010) 1227-1233.

[14] X. Pang, F. Li, S. Huang, Z. Yang, Q. Mo, L. Huang, W. Xu, L. Chen, X. Li, Electrostatically mediated layer-by-layer assembly of nitrogen-doped graphene/PDDA/gold nanoparticle composites for electrochemical detection of uric acid, Anal. Bioanal. Chem. (2019) 1-12.

[15] Y. Wang, Y. Shao, D.W. Matson, J. Li, Y. Lin, Nitrogen-doped graphene and its application in electrochemical biosensing, ACS. Nano. 4(4) (2010) 1790-1798.

[16] L.-M. Lu, H.-B. Li, F. Qu, X.-B. Zhang, G.-L. Shen, R.-Q. Yu, In situ synthesis of palladium nanoparticle–graphene nanohybrids and their application in nonenzymatic glucose biosensors, Biosens. Bioelectron. 26(8) (2011) 3500-3504.

[17] S. Zhuo, J. Fang, C. Zhu, J. Du, Preparation of palladium/carbon dot composites as efficient peroxidase mimics for $H_2O_2$ and glucose assay, Anal. Bioanal. Chem. (2019) 1-10.

[18] A. Aziz, M. Asif, G. Ashraf, M. Azeem, I. Majeed, M. Ajmal, J. Wang, H. Liu, Advancements in electrochemical sensing of hydrogen peroxide, glucose and dopamine by using 2D nanoarchitectures of layered double hydroxides or metal dichalcogenides. A review, Mikrochim. Acta. 186(10) (2019) 671.

[19] L. Fernández, C. Borrás, J. Mostany, B. Scharifker, 4. Layered Double Hydroxides for electrochemical sensing application.

[20] S. Samuei, J. Fakkar, Z. Rezvani, A. Shomali, B. Habibi, Synthesis and characterization of graphene quantum dots/CoNiAl-layered double-hydroxide nanocomposite: Application as a glucose sensor, Anal. Biochem. 521 (2017) 31-39.

[21] J. Yuan, S. Xu, H.-Y. Zeng, X. Cao, A.D. Pan, G.-F. Xiao, P.-X. Ding, Hydrogen peroxide biosensor based on chitosan/2D layered double hydroxide composite for the determination of $H_2O_2$, Bioelectrochemistry. 123 (2018) 94-102.

[22] E. Asadian, S. Shahrokhian, A.I. Zad, Highly sensitive nonenzymetic glucose sensing platform based on MOF-derived NiCo LDH nanosheets/graphene nanoribbons composite, J. Electroanal. Chem. 808 (2018) 114-123.

[23] Q. Wang, X. Cui, J. Chen, X. Zheng, C. Liu, T. Xue, H. Wang, Z. Jin, L. Qiao, W. Zheng, Well-dispersed palladium nanoparticles on graphene oxide as a non-enzymatic glucose sensor, RSC. Adv. 2(15) (2012) 6245-6249.

[24] A. Eshghi, Graphene/Ni–Fe layered double hydroxide nano composites as advanced electrode materials for glucose electro oxidation, Int, J. Hydrogen. Energy. 42(22) (2017) 15064-15072.

[25] S. Fu, G. Fan, L. Yang, F. Li, Non-enzymatic glucose sensor based on Au nanoparticles decorated ternary Ni-Al layered double hydroxide/single-walled carbon nanotubes/graphene nanocomposite, Electrochimica acta 152 (2015) 146-154.

[26] R. Salahandish, A. Ghaffarinejad, E. Omidinia, H. Zargartalebi, K. Majidzadeh-A, S.M. Naghib, A. Sanati-Nezhad, Label-free ultrasensitive detection of breast cancer miRNA-21 biomarker employing electrochemical nano-genosensor based on sandwiched AgNPs in PANI and N-doped graphene, Biosens. Bioelectron. 120 (2018) 129-136.

[27] E. Scavetta, A. Mignani, D. Prandstraller, D. Tonelli, Electrosynthesis of thin films of Ni, Al hydrotalcite like compounds, Chem. Mater. 19(18) (2007) 4523-4529.

[28] Y. Wang, Y. Rui, F. Li, M. Li, Electrodeposition of nickel hexacyanoferrate/layered double hydroxide hybrid film on the gold electrode and its application in the electroanalysis of ascorbic acid, Electrochim. Acta. 117 (2014) 398-404.

[29] C. Hu, J. Dong, T. Wang, R. Liu, H. Liu, J. Qu, Nitrate electro-sorption/reduction in capacitive deionization using a novel Pd/NiAl-layered metal oxide film electrode, Chem. Eng. J. 335 (2018) 475-482.

[30] W. Zheng, S. Sun, Y. Xu, R. Yu, H. Li, Facile synthesis of NiAl-LDH/$MnO_2$ and NiFe-LDH/$MnO_2$ composites for high-performance asymmetric supercapacitors, J. Alloys. Compd. 768 (2018) 240-248.

[31] C. Ghiabi, A. Ghaffarinejad, H. Kazemi, R. Salahandish, In situ, one-step and co-electrodeposition of graphene supported dendritic and spherical nano-palladium-silver bimetallic catalyst on carbon cloth for electrooxidation of methanol in alkaline media, Renew. Energy. 126 (2018) 1085-1092.

[32] K. Ramachandran, K.J. Babu, Ni-Co bimetal nanowires filled multiwalled carbon nanotubes for the highly sensitive and selective non-enzymatic glucose sensor applications, Sci. Rep. 6 (2016) 36583.

[33] K.E. Toghill, R.G. Compton, Electrochemical non-enzymatic glucose sensors: a perspective and an evaluation, Int. J. Electrochem. Sci. 5(9) (2010) 1246-1301.

[34] J. Chen, Q. Sheng, Y. Wang, J. Zheng, Dispersed Nickel Nanoparticles on Flower- like Layered Nickel- Cobalt Double Hydroxides for Non- enzymic Amperometric Sensing of Glucose, Electroanalysis. 28(5) (2016) 979-984.

[35] B. Hai, Y. Zou, Carbon cloth supported NiAl-layered double hydroxides for flexible application and highly sensitive electrochemical sensors, Sens. Actuators. B. Chem. 208 (2015) 143-150.

[36] X. Li, J. Liu, X. Ji, J. Jiang, R. Ding, Y. Hu, A. Hu, X. Huang, Ni/Al layered double hydroxide nanosheet film grown directly on Ti substrate and its application for a nonenzymatic glucose sensor, Sens. Actuators. B. Chem. 147(1) (2010) 241-247.

[37] Y. Lu, B. Jiang, L. Fang, S. Fan, F. Wu, B. Hu, F. Meng, Highly sensitive nonenzymatic glucose sensor based on 3D ultrathin NiFe layered double hydroxide nanosheets, Electroanalysis. 29(7) (2017) 1755-1761.

[38] H. Ai, X. Huang, Z. Zhu, J. Liu, Q. Chi, Y. Li, Z. Li, X. Ji, A novel glucose sensor based on monodispersed Ni/Al layered double hydroxide and chitosan, Biosens. Bioelectron. 24(4) (2008) 1048-1052.

[39] J. Xu, X. Qiao, M. Arsalan, N. Cheng, W. Cao, T. Yue, Q. Sheng, J. Zheng, Preparation of one dimensional silver nanowire/nickel-cobalt layered double hydroxide and its electrocatalysis of glucose, J. Electroanal. Chem. 823 (2018) 315-321.

[40] G. Ni, J. Cheng, X. Dai, Z. Guo, X. Ling, T. Yu, Z. Sun, Integrating Ultrathin Polypyrrole Framework on Nickel- Cobalt Layered Double Hydroxide as an Amperometric Sensor for Non-enzymatic Glucose Determination, Electroanalysis. 30(10) (2018) 2366-2373.

[41] D. Chu, F. Li, X. Song, H. Ma, L. Tan, H. Pang, X. Wang, D. Guo, B. Xiao, A novel dual-tasking hollow cube $NiFe_2O_4$-NiCo-LDH@ rGO hierarchical material for high preformance supercapacitor and glucose sensor, J. Colloid. Interface. Sci. 568 (2020) 130-138.

## Figures Captions

Fig. 1 Scheme of the glucose sensor fabrication process.

Fig. 2 XPS spectra of (A) Pd *3d*, (B) Ni *2p*, and (C) Al *2p* in GS/NFG/Pd-NiAl-LDH electrode.

Fig. 3 (A) SEM image of GS/NFG. (B) FE-SEM images of GS/NFG/NiAl-LDH at 60 s of electrodeposition time and (C) at 90 s. (D, E and F) FE-SEM images of GS/NFG/Pd-NiAl-LDH. (G) Elemental mappings of C, O, Ni, Al and Pd of GS/NFG/Pd-NiAl-LDH.

Fig. 4 (A) LSV of different modified layers including, (a) bare GS, (b) GS/NFG, (c) GS/NiAl-LDH, (d) GS/NFG/NiAl-LDH, (e) GS/Pd-NiAl-LDH and (f) GS/NFG/Pd-NiAl-LDH in 0.01 M PBS solution

containing 2.5 mM of $[Fe(CN)_6]^{3-/4-}$. (B) The EIS measurements of different modified layers in 0.01 M PBS solution containing 2.5 mM of $[Fe(CN)_6]^{3-/4-}$.

Fig. 5 (A) LSV of GS/NFG/Pd-NiAl-LDH electrode in 0.1 M NaOH containing 10 mM glucose at different scan rates from 10 to 200 $mV.s^{-1}$. (B) Plot of $j_{pa}$ versus square root of scan rate. (C) Current density of GS/NFG/Pd-NiAl-LDH electrode by LSV in the 0.01 M PBS solution containing 10 mM of glucose at different pH values. (D) Current density response of GS/NFG/Pd-NiAl-LDH electrode recorded by CA at 80 s in 0.01 M PBS solution contain 10 mM of glucose at different pH values. (E) Chronoamperograms, and (F) current density values of GS/NFG/Pd-NiAl-LDH electrode recorded by CA at 80 s in 0.1 M NaOH solution containing 10 mM glucose at different applied potentials from 0.4 V to 0.6 V for 130 s.

Fig. 6 LSV curves (A) and calibration plot (B) of GS/NFG/Pd-NiAl-LDH electrode in 0.1 M NaOH contain different concentration of glucose from 0.1 - 10 mM at 20 $mV.s^{-1}$. The amperometric response (C) and calibration plot (D) of GS/NFG/Pd-NiAl-LDH electrode in 0.1 M NaOH containing different concentrations of glucose from 0.0005 - 10 mM at the applied potential of 0.5 V.

Fig. 7 (A) Interference test of GS/NFG/Pd-NiAl-LDH electrode with successful injection of glucose and the interferences in 0.1 M NaOH at an applied potential of 0.5 V. (B) Real sample study with GS/NFG/Pd-NiAl-LDH electrode by CA technique in serum, plasma, and blood samples containing 1 and 3 mM of glucose and 0.1 M NaOH at an applied potential of 0.5 V.

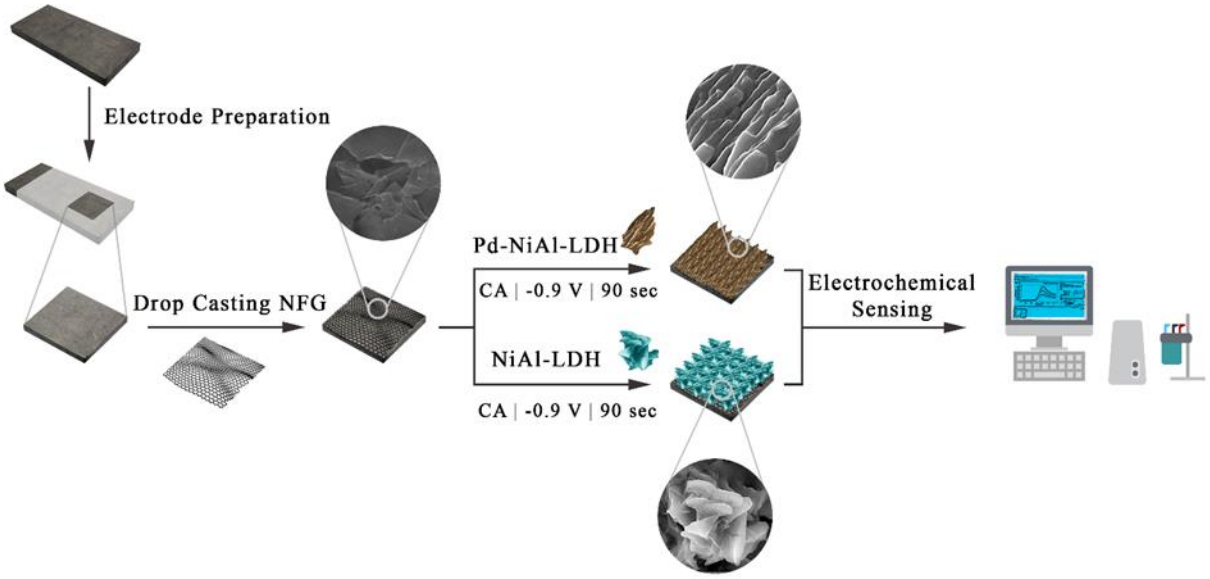


**Fig. 1**

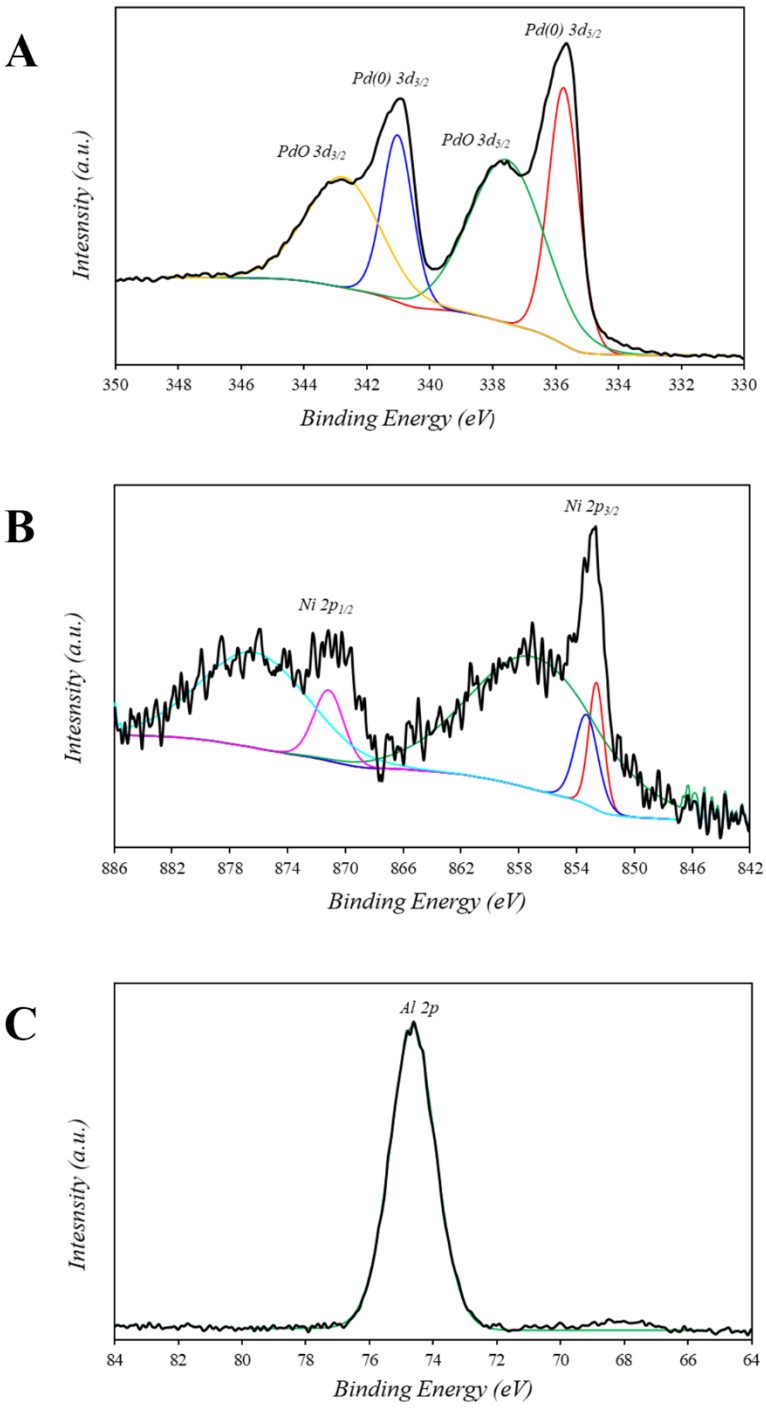
A
Pd(0) 3d5/2
Pd(0) 3d3/2
PdO 3d5/2
PdO 3d3/2
Intesnsity (a.u.)
350 348 346 344 342 340 338 336 334 332 330
Binding Energy (eV)
B
Ni 2p3/2
Ni 2p1/2
Intesnsity (a.u.)
886 882 878 874 870 866 862 858 854 850 846 842
Binding Energy (eV)
C
Al 2p
Intesnsity (a.u.)
84 82 80 78 76 74 72 70 68 66 64
Binding Energy (eV)

**Fig. 2**

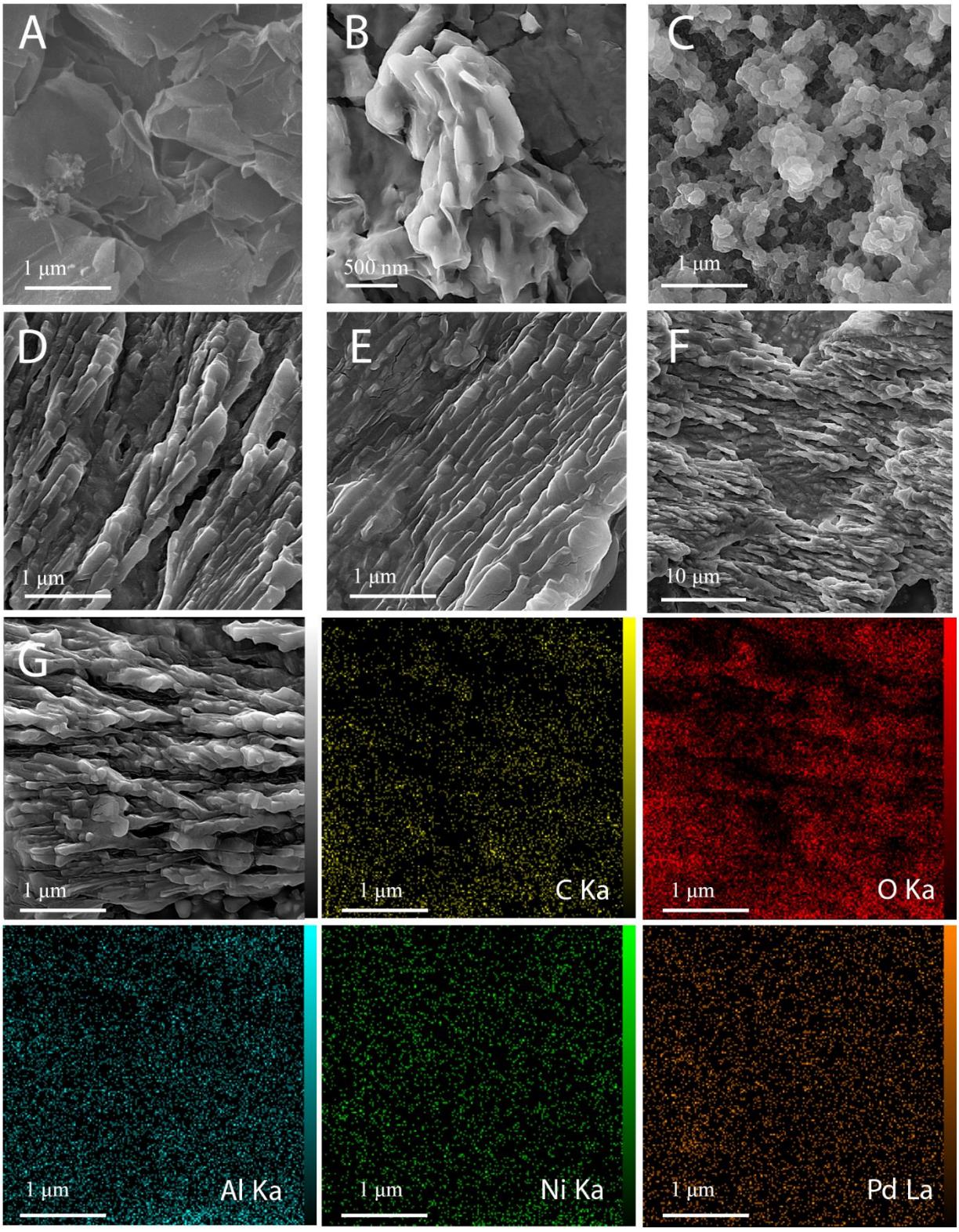
A
1 µm
B
500 nm
C
1 µm
D
1 µm
E
1 µm
F
10 µm
G
1 µm
1 µm
C Ka
1 µm
O Ka
1 µm
Al Ka
1 µm
Ni Ka
1 µm
Pd La

**Fig. 3**

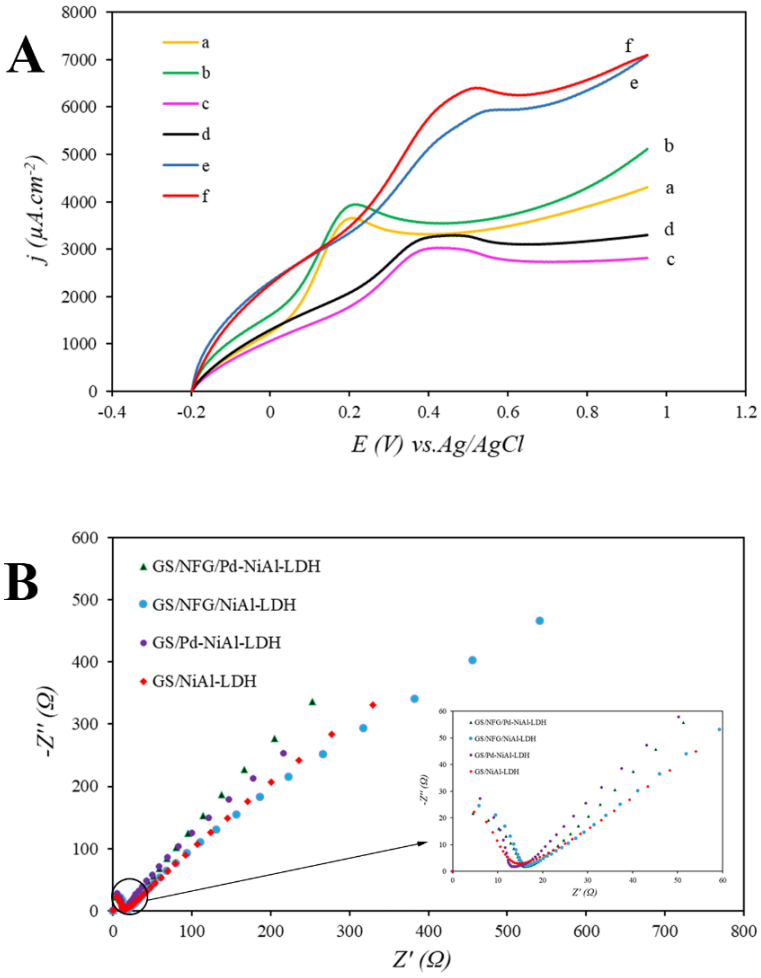
A
a
b
c
d
e
f
j (μA.cm⁻²)
E (V) vs.Ag/AgCl
B
GS/NFG/Pd-NiAl-LDH
GS/NFG/NiAl-LDH
GS/Pd-NiAl-LDH
GS/NiAl-LDH
-Z'' (Ω)
Z' (Ω)

**Fig. 4**

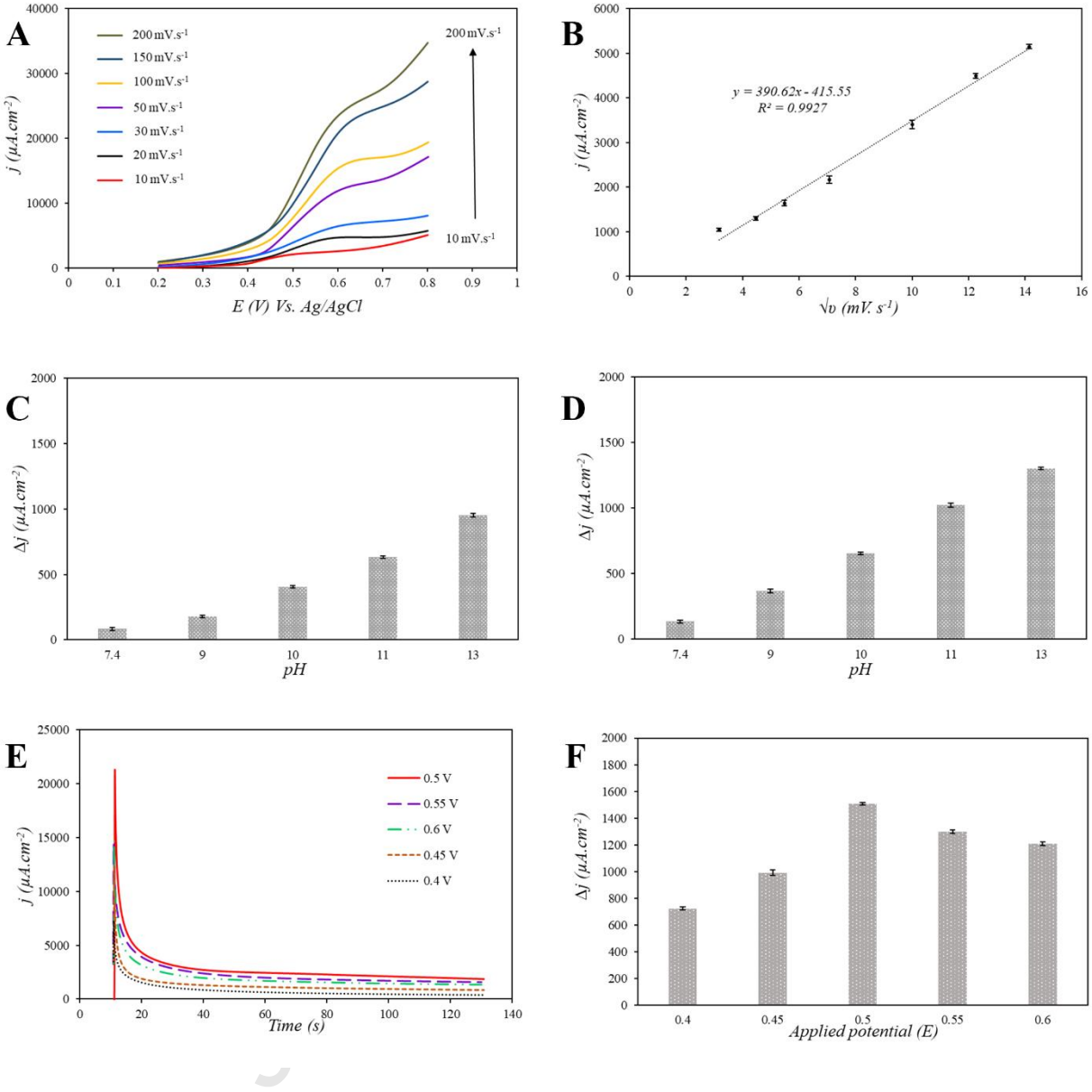
A
200 mV.s-1
150 mV.s-1
100 mV.s-1
50 mV.s-1
30 mV.s-1
20 mV.s-1
10 mV.s-1
200 mV.s-1
10 mV.s-1
j (µA.cm-2)
E (V) Vs. Ag/AgCl
B
y = 390.62x - 415.55
R² = 0.9927
j (µA.cm-2)
√υ (mV. s-1)
C
Δj (µA.cm-2)
pH
D
Δj (µA.cm-2)
pH
E
0.5 V
0.55 V
0.6 V
0.45 V
0.4 V
j (µA.cm-2)
Time (s)
F
Δj (µA.cm-2)
Applied potential (E)

**Fig. 5**

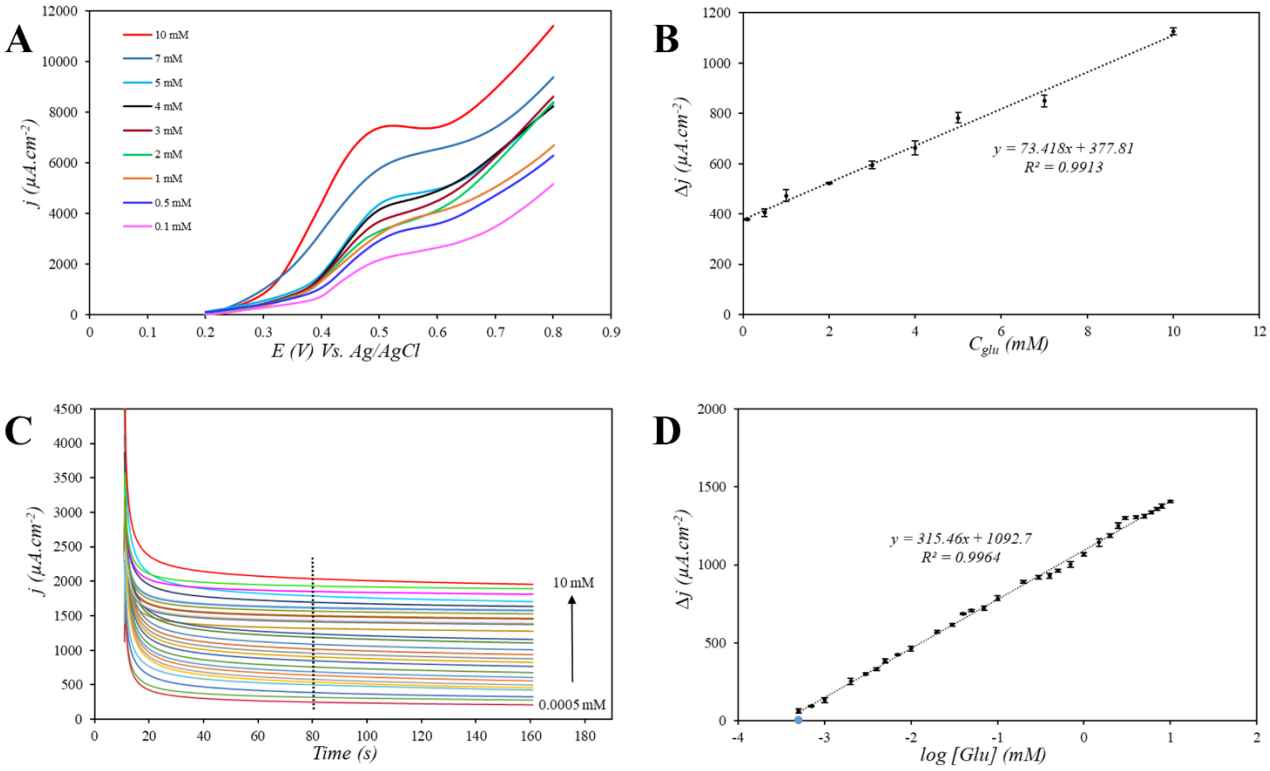


**Fig. 6**

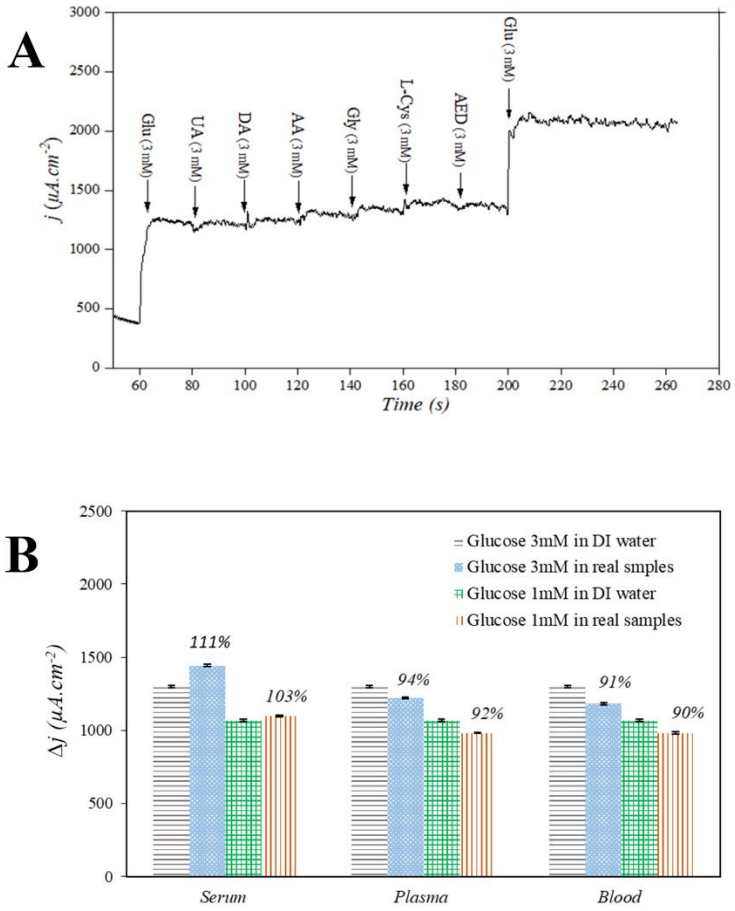
A
Glu (3 mM)
UA (3 mM)
DA (3 mM)
AA (3 mM)
Gly (3 mM)
L-Cys (3 mM)
AED (3 mM)
Glu (3 mM)
j (μA.cm-2)
Time (s)
B
Glucose 3mM in DI water
Glucose 3mM in real smples
Glucose 1mM in DI water
Glucose 1mM in real samples
Δj (μA.cm-2)
111%
103%
94%
92%
91%
90%
Serum
Plasma
Blood

**Fig. 7**

## Credit Author Statement

**Niusha Shishegari**: Validation, Formal analysis, Writing - Original Draft

**Abbas Sabahi:** Conceptualization, Validation, Formal analysis, Writing - Original Draft

**Faranak Manteghi:** Resources, Writing - Review & Editing, Supervision, Funding acquisition

**Ali Ghaffarinejad:** Investigation, Resources, Writing - Review & Editing, Project administration, Funding acquisition

**Zari Tehrani:** Resources, Investigation

**Declaration of interests**

☒ The authors declare that they have no known competing financial interests or personal relationships that could have appeared to influence the work reported in this paper.

☐The authors declare the following financial interests/personal relationships which may be considered as potential competing interests:

## Highlights:

- The Pd-NiAl-LDH nano-composite was prepared via one-step electrodeposition process
- The composite had an excellent electroactivity toward glucose oxidation
- NFG prepared a large surface area for electrodeposition of Ni and Pd active centers
- The reproducibility, repeatability and stability of the proposed sensor was good
- Fabricated sensor has an acceptable performance in human serum, plasma and blood